Contrib Mineral Petrol (1997) 128: 287–301

M.V. Portnyagin · L.V. Danyushevsky · V.S. Kamenetsky

Coexistence of two distinct mantle sources during formation of ophiolites: a case study of primitive pillow-lavas from the lowest part of the volcanic section of the Troodos Ophiolite, Cyprus

Received: 20 May 1996 / Accepted: 25 March 1997

Abstract We present a detailed mineralogical, petrological and melt inclusion study of unusually fresh, primitive olivine + clinopyroxene phyric Lower Pillow Lavas (LPL) found near Analiondas village in the northeastern part of the Troodos ophiolite (Cyprus). Olivine phenocrysts in these primitive LPL show a wide compositional range ($Fo_{82–92}$) and have higher CaO contents than those from the Upper Pillow Lavas (UPL). Cr-spinel inclusions in olivine are significantly less Cr-rich (Cr/Cr + Al = 28–67 mol%) compared to those from the UPL (Cr# = 70–80). These features reflect differences in melt compositions between primitive LPL and the UPL, namely higher CaO and Al_2O_3 and lower FeO* compared to the UPL at a given MgO. LPL parental melts (in equilibrium with Fo_{92}) had ~10.5 wt% MgO and crystallization temperatures ~1210 °C, which are significantly lower than those previously published for the UPL (14–15 wt% MgO and ~1300 °C for Fo_{92}). The fractionation path of LPL parental melts is also different from that of the UPL. It is characterized initially by olivine + clinopyroxene cotectic crystallization joined by plagioclase at ~9 wt% MgO, whereas UPL parental melts experienced a substantial interval of olivine-only crystallization. Primitive LPL melts were formed from a mantle source which was more fertile than that of tholeiites from well-developed intra-oceanic arcs, but broadly similar in its fertility to that of Mid-Ocean Ridge Basalt (MORB) and Back Arc Basin Basalts (BABB). The higher degrees of melting during formation of the LPL primary melts compared to average MORB were caused by the presence of subduction-related components (H_2O). Our new data on the LPL coupled with existing data for the UPL support the existing idea that the LPL and UPL primary melts originated from distinct mantle sources, which cannot be related by progressive source depletion. Temperature differences between these sources (~150 °C), their position in the mantle (~10 kbar for the colder LPL source vs 15–18 kbar for the UPL source), and temporal succession of Troodos volcanism, all cannot be reconciled in the framework of existing models of mantle wedge processes, thermal structure and evolution, if a single mantle source is invoked. Possible tectonic settings for the origin of the Troodos ophiolite (forearc regions of intra-oceanic island arc, propagation of backarc spreading into arc lithosphere) are discussed.

M.V. Portnyagin
Vernadsky Institute of Geochemistry, Kosigin str.,
19 Moscow 117975, Russia

L.V. Danyushevsky (✉) · V.S. Kamenetsky
Dept. of Geology, University of Tasmania,
GPO Box 252-79, Hobart, 7001, Australia
Tel. 61-3-62262469, fax. 61-3-62232547,
email: L.Dan@utas.edu.au

V.S. Kamenetsky
Research School of Earth Sciences,
The Australian National University,
Canberra, ACT 0200, Australia

Editorial responsibility: T.L. Grove

Introduction

To reconcile structural evidence for an extensional regime in supra-subduction zone (SSZ) ophiolites (e.g., Troodos, Oman) with subduction-related geochemical signatures of their magmatic suites, Pearce et al. (1984) proposed that such ophiolites were formed by sea-floor spreading during the initial stages of subduction. This idea has been supported by recent studies of the Western Pacific forearc assemblages (e.g., Stern and Bloomer 1992; Pearce et al. 1992; Taylor 1992; Taylor and Nesbitt 1995; Bloomer et al. 1995), which have suggested that forearc suites were also formed in an extensional environment during or soon after the initiation of subduction. These new findings provided an explanation for a similarity of rock types (i.e., lavas, dykes and intrusives within boninite-arc tholeiite compositional spectrum, and peridotites) found in modern forearcs and SSZ

ophiolites (e.g., Bloomer and Hawkins 1983; Sharaskin et al. 1983), and it has been proposed that these forearcs are the best modern analogs for SSZ ophiolites (e.g., Bloomer et al. 1995). However, the association of variably evolved tholeiites with strong "arc" affinities and more primitive boninite and boninite-like lavas has also been described at presently active spreading centres propagating towards the Tonga arc in the southern and northern parts of the Lau Backarc Basin (southern tip of the Valu Fa Ridge; Frenzel et al. 1990; Vallier et al. 1991; King's Triple Junction: Falloon and Crawford 1991; Falloon et al. 1992).

Detailed understanding of magma genesis in variety of extensional tectonic settings within present-day SSZ is hampered by a paucity of data, which mainly derives from a limited number of drill-holes and dredges. In this respect, the study of well-preserved and exposed suprasubduction zone ophiolites, such as Troodos (e.g., Schmincke et al. 1983; Robinson et al. 1983; McCulloch and Cameron 1983; Rautenschlein et al. 1985; Cameron 1985; Rogers et al. 1989), may provide additional constraints on the evolution of the SSZ magmatism in extensional settings.

The Troodos Ophiolite has been extensively studied during the last four decades. The Troodos lava complex has been divided into the Lower and Upper Pillow Lava suites (LPL and UPL) (e.g., Gass and Smewing 1973). The younger UPL are composed of basaltic andesites and basalts with common picritic lava flows and dykes (e.g., Schmincke et al. 1983). Despite certain mineralogical and geochemical differences among UPL rocks which led to their division into several types (e.g., Cameron 1985), the UPL as a whole represent a distinct magmatic group. They are characterized by the presence of high-forsteritic olivine phenocrysts (up to Fo_{94}), chromium-rich spinel {Cr# = 100*[Cr/(Cr + Al)] = 65–80}, an absence of plagioclase phenocrysts in all rock types but basaltic andesites, low TiO_2 (<1 wt%) and high H_2O contents (~2 wt%), and trace element contents typical of subduction-related magmas (e.g., McCulloch and Cameron 1983; Rautenschlein et al. 1985; Cameron 1985; Sobolev et al. 1993). The petrological and geochemical features of the UPL have been used as a reference type for the high-Ca boninite magmatic suite (Crawford et al. 1989).

Unlike the UPL, the older LPL are broadly andesitic, resembling evolved island-arc tholeiites (e.g., Robinson et al. 1983; Schmincke et al. 1983). However, recent studies have revealed that the lowest parts of the LPL, representing the earliest recognized Troodos volcanic episode, are composed of relatively low-Ti lavas more primitive than later LPL (Bednarz et al. 1991; Sobolev et al. 1993; Bednarz and Schmincke 1994). Andesites and dacites are interpreted to be directly related to those more primitive LPL by open-system fractional crystallization (Bednarz and Schmincke 1994).

It has been argued that the UPL and the least-evolved LPL are unlikely to be connected by magmatic differentiation (e.g., Bednarz and Schmincke 1994), with the difference in stratigraphic position, and chemical and modal composition differences of the LPL and UPL being invoked to validate the genetic discontinuity between these magmatic suites. The successive formation of the LPL and UPL has been explained by progressive continuous (Wood 1979; Bednarz and Schmincke 1994) or multistage (Duncan and Green 1980, 1987) depletion of a single mantle source.

Detailed information on the least evolved LPL has been lacking due to their pervasive alteration, and in this paper we present a petrological and melt inclusion study of well-preserved primitive LPL found near Analiondas village in the northeastern part of Troodos. We demonstrate that these early-formed Troodos primitive lavas are indeed parental to the LPL andesites and dacites, and that they differ substantially from the typical boninite-like UPL. Moreover, our results support the idea that the LPL and UPL primary melts originated from distinct mantle sources (Sobolev et al. 1993) which cannot be related by progressive source depletion. We also discuss possible tectonic settings for the origin of the Troodos ophiolite.

Geological setting

Sequences of lavas more primitive than the common LPL have been found in the lowest parts of the LPL sequence, overlying the Basal Group in some areas (Bednarz and Schmincke 1994; Taylor 1987). The lavas are usually aphyric. If porphyritic, the modal phenocryst composition of these lavas is similar to the UPL, but usually contains higher plagioclase abundances (Bednarz and Schmincke 1994). These primitive lower parts of the LPL section are usually strongly altered. A relatively fresh and thick sequence has been described only in the vicinity of Analiondas village in northeastern Troodos (Boyle and Robertson 1984; Taylor 1987).

The geological setting of the Analiondas area is shown on Fig. 1. The exposed thickness of the LPL in this region is ~1.5 km. To the northeast, this suite bounds the UPL "classic" locality in the vicinity of Margi village (e.g., Gass 1958); to the southwest, it abuts the Dyke Complex. The suite is composed of lava flows 1–5 m thick with subordinate pillow lavas and hyaloclastites. Most of the lavas are aphyric and strongly altered. The suite is cut by numerous subvertical northeast-trending faults, and is intruded by aphyric or sometimes olivine + clinopyroxene-phyric dikes normally 1–3 m thick.

A 500 m long outcrop of olivine + clinopyroxene-phyric primitive pillow lavas associated with hyaloclastites and interlayered with LPL andesites and dacites lava flows has been found along the east side of the Analiondas-Kataliondas road (Fig. 1). Pillow-lava layers are 1–1.5 m thick and the entire succession of pillow lavas and lava flows is concordant with the LPL in the area. The southwest end of this sequence is cut by an

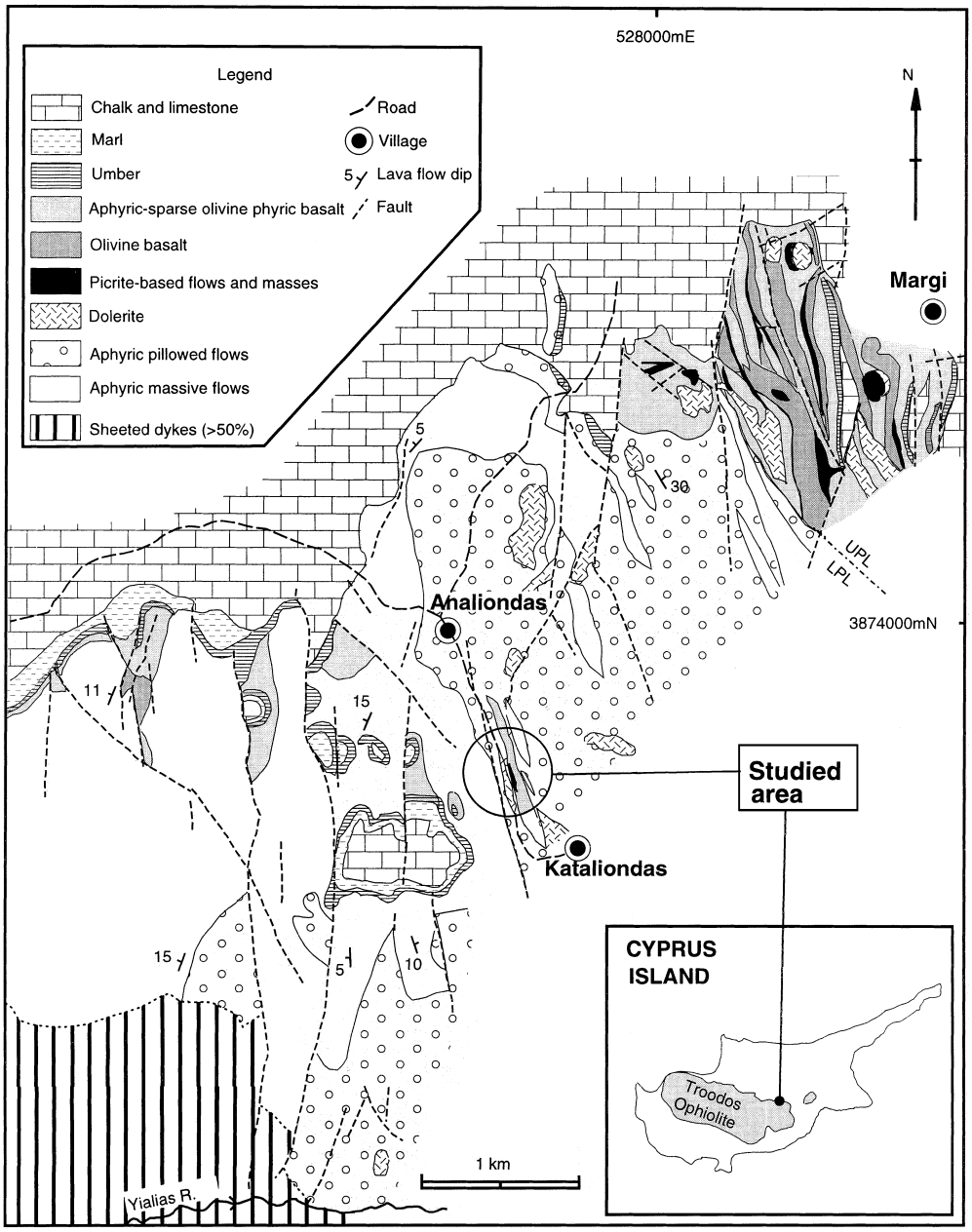

Fig. 1 Geological map of the Analiondas-Kataliondas-Margi area, northeastern Troodos (after Taylor 1987). Coordinate ticks indicate the 1000 metre Universal Transverse Mercator Grid, Zone 36, International Spheroid, European Datum. 1 km scale bar is shown

aphyric dike; to the northeast, it is stratigraphically overlapped by aphyric LPL. Pillows are normally ~1 m in diameter, and vary in modal composition from phenocryst-enriched in the inner parts to almost aphyric in quenched margins. Pillows are usually less altered than interbedded massive flows. In general, these lavas resemble in their appearance picrites and glassy basalts from UPL in the same volcanic section described by Gass (1958), but are more enriched in clinopyroxene phenocrysts.

Petrography and chemistry

Primitive pillow lavas from the Analiondas area are aphyric to strongly olivine + clinopyroxene-phyric rocks with quenched glass margins (Table 1). Cr-spinel was also found as isolated phenocrysts. Phenocrysts make up to 30% of the inner parts of some pillows (sample TRD-150), and they gradually decrease in abundance to 5–10% towards pillow rims. Plagioclase is present as microphenocrysts (<1 mm). Doleritic groundmass in picrites is composed of elongated skeletal laths of plagioclase and clinopyroxene and equigranular Ti-magnetite. Interstitial glass has been devitrified and replaced by secondary minerals. Hyaloclastites associated with pillow lavas also contain olivine and clinopyroxene phenocrysts.

The interlayered, more typical LPL lavas are aphyric andesites and sparsely clinopyroxene-phyric basaltic andesites. The groundmass consists of small laths of plagioclase, clinopyroxene and Ti-magnetite.

The composition of the most evolved pillow-rim glass (TRD-149) falls within the field of the LPL andesites and dacites; basaltic andesite glasses (TRV-49,53) are similar to the typical UPL glasses, whereas the most Mg-rich glasses from picritic pillows and hyaloclastites (TRD-147, TRV-48) are unique among Troodos glass compositions (Fig. 2). The MgO content of these glasses falls within

Table 1 The compositions of Analiondas rocks and glasses[a] (*p* pillow lava, *s* sheet flow, *h* hyaloclastite, *d* dyke, *WR* whole rock, *GL* glass)

Number	TRD-150	TRV-57	TRD-148	TRD-147	TRD-149	TRD-149	TRD-152	TRD-151	TRV-48	TRV-49	TRV-53
Lithology	p	p	p	p	s	s	p	d	h	s	d
	WR	WR	WR	GL	WR	GL	WR	WR	GL	GL	GL
SiO_2	44.42	43.76	42.81	51.41	51.92	55.50	46.36	50.44	50.84	53.32	54.55
TiO_2	0.34	0.3	0.4	0.49	1.03	1.05	0.66	0.61	0.41	0.59	0.63
Al_2O_3	10.25	9.34	12.45	15.91	15.47	15.19	15.73	15.09	16.15	16.03	15.76
FeO[b]	8.16	8.05	6.29	6.81	8.7	10.41	10.32	7.5	7.36	7.88	8.4
MnO	0.16	0.144	0.15	0.14	0.14	0.18	0.15	0.15	0.14	0.17	0.19
MgO	22.23	22.97	9.74	8.40	5.72	3.83	7.03	6.08	8.34	6.76	6.02
CaO	7.96	7.19	17.91	13.90	7.69	8.73	7.82	9.78	13.69	11.27	10.23
Na_2O	0.51	0.42	0.80	1.55	2.55	2.18	1.32	1.55	1.37	1.98	1.80
K_2O	0.07	0.11	0.18	0.12	0.3	0.2	2.79	2.97	0.09	0.17	0.19
P_2O_5	0.05		0.04	0.05	0.11	0.09	0.13	0.07	0.04	0.06	0.06
Cr_2O_3	0.14			0.04	0.02	0.03	0.04	0.02	0.06	0.02	0.01
LOI	5.9	8.1	8.5	1.53[c]	5.65		6.55	6.65			
Total	100.19	100.38	99.27	99.79	99.30	97.39	98.90	100.91	98.49	98.25	97.84
La	0.80	0.63		1.00	2.48						
Ce	2.00	1.5		3.18	6.5						
Nd		1.7		2.49							
Sm	0.713	0.64		0.96	2.20						
Eu	0.25	0.23		0.36	0.94						
Tb	0.174	0.18			0.57						
Dy				1.9							
Er				1.25							
Yb	0.83	0.8		1.36	2.67						
Lu	0.13	0.14									
Ta	0.02				0.079						
Nb	< 0.7	< 0.5	5	0.34	< 2		7	9			
Zr	14	12	25	20	58		28	36			
Hf	0.38				2.48						
Y	7.7	7.4	14	11.2	28		34	18			
V	136		174		346		434	237			
Cs	0.065				0.09						
Rb	0.91		5		2.9		24	13			
Sr	38		83	62	109		93	85			
Ba	3.1		22	11.4	25		63	93			
Th	0.147				0.309						
U	0.036				0.15						
Sc	26.7		35		34.9		49	37			
Ni	605		268		24		85	56			
Cr	1498		803	389	15		364	121			
Co	72		61		35.5		48	51			
Zn	59		55		96		84	52			
Cu	55		63		95		83	161			
Ga	9		11		16		12	14			
Mo	8		10		8		11	6			

[a] Major element whole rock analyses and underlined trace elements by XRF at Vernadsky Institute, Moscow and GEOMAR, Kiel, Germany using a Philips PW-1400 spectrometer; other trace elements in rock samples by INAA at CRPG, Nancy, France; glass major elements by electron microprobe Cameca SX50 at GEOMAR, Kiel using routine operating conditions and basaltic glass USNM 111240/52 (Jarosevich et al. 1980) as a standard; glass trace elements by ion microprobe Cameca IMS4f (Microelectronics Inst., Yaroslavl, Russia), and H_2O by ion microprobe Cameca IMS-3f (CRPG, Nancy, France). The details of the technique are given in Sobolev and Chaussidon (1996)

[b] Total iron as FeO

[c] H_2O in glass

the MgO range of the UPL glasses, however they have higher Al_2O_3 and CaO and lower FeO* abundances compared to all UPL glasses at a given MgO content. Unlike Al_2O_3, CaO, and FeO*, contents of Na_2O, TiO_2 and SiO_2 differ between the UPL types, and Analiondas glasses fall within the range of the UPL for these elements. The H_2O (not shown) and K_2O contents are also similar to the UPL glasses. Picritic compositions (TRD-150, TRV-57) are generally similar to picritic UPL from the Margi area (Sobolev et al. 1993). A strong enrichment of some samples in CaO (picrite TRD-148) and K_2O (basalts TRD-151,152) reflects low-temperature alteration.

The trace element compositions of selected samples are shown in Table 1 and Fig. 3. All samples are characterized by similar subparallel shapes of normalized patterns with higher ratios of Large Ion Lithophile Elements (LILE) to Rare Earth Elements (REE), and lower ratios of High Field Strength Elements (HFSE) to REE (except (Ti/REE) compared to Normal Mid Ocean Ridge Basalt (NMORB). These compositions are typical for Troodos lavas (e.g., Rautenschlein et al. 1985), and together with elevated H_2O contents, manifest their SSZ origin. The incompatible element abundances correlate negatively with MgO and for most elements may be accounted for by processes of crystal fractionation/accumulation.

Trace element abundances in basalts and picrites are close to those in the type I UPL of Cameron (1985). Andesitic sample

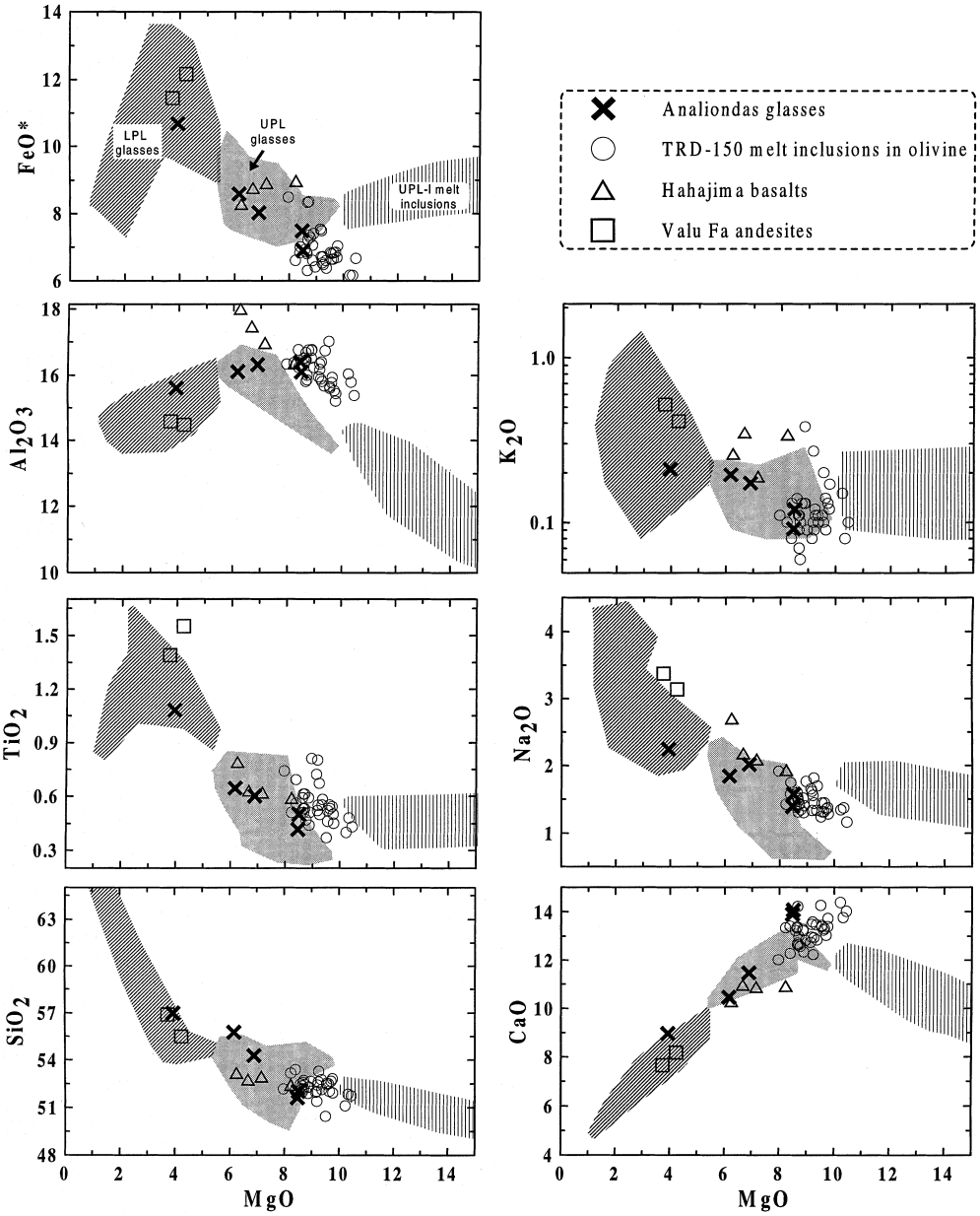

Fig. 2 Major element compositions of pillow-rim glasses and homogenized melt inclusions in olivine from Analiondas picrite TRD-150. Fields of types I, II and III UPL glasses and LPL glasses after (Robinson et al. 1983; Rautenschlein et al. 1985; Flower and Levine 1987; Taylor 1987; Thy and Xenophontos 1991; Bailey et al. 1991; Sobolev et al. 1993; Bednarz and Schmincke 1994; Portnyagin unpublished data). The field of homogenized melt inclusions in olivine phenocrysts from type I UPL picrites after Sobolev et al. (1993). Compositions of Bonin forearc tholeiites (Hahajima Island) after Taylor and Nesbitt (1995). Note that high Al_2O_3 contents of these tholeiites are not representative of magma compositions and reflect plagioclase accumulation (Taylor and Nesbitt 1995). Valu Fa Ridge andesites after Vallier et al. (1991). All compositions are normalized to 100 wt% anhydrous. Iron content in melt inclusions is corrected to account for the 'iron loss' (see text for details)

TRD-149 falls within the compositional range of the LPL from other areas. All rocks studied have very low Ta(Nb)/LREE (Light Rare Earth Element) values, which are a characteristic feature of both the LPL and the least depleted (type I) UPL (e.g., Bednarz and Schmincke 1994).

In summary, major element compositions of primitive Analiondas rocks and glasses show some significant differences compared to the UPL, whereas their trace element contents are similar to the UPL, but share some specific features with the LPL andesites and dacites. Compositions of evolved Analiondas samples resemble LPL from other areas.

Mineralogy of picrite TRD-150

Olivine phenocrysts have a range of Mg# [100*Mg/(Mg + Fe)] from 83 to 92 (Table 2). Most of the olivine phenocryst population have Fo > 88. Such large variations of Fo between olivine phenocrysts in a single rock indicate that they could not have crystallized from a single melt composition, and may represent snapshots of various stages of the crystallization history of the parent magma. The range of Fo observed in this sample is larger than the entire range of olivine phenocryst compositions from UPL picrites (87–94, e.g., Sobolev et al. 1993). The range of Fo in TRD-150 extends to significantly less magnesian values than those found in UPL picrites, and the very magnesian compositions ($> Fo_{92}$) common in UPL picrites (e.g., Sobolev et al. 1993) have not been found in this sample. CaO contents in TRD-150 olivine are in the range 0.22–0.35 wt% in Fo > 90 and gradually decrease to < 0.2 wt% in $Fo_{83–86}$. The CaO contents of olivine from this rock are generally higher than those of the UPL olivine (0.16–0.28 wt% in $Fo_{89–94}$).

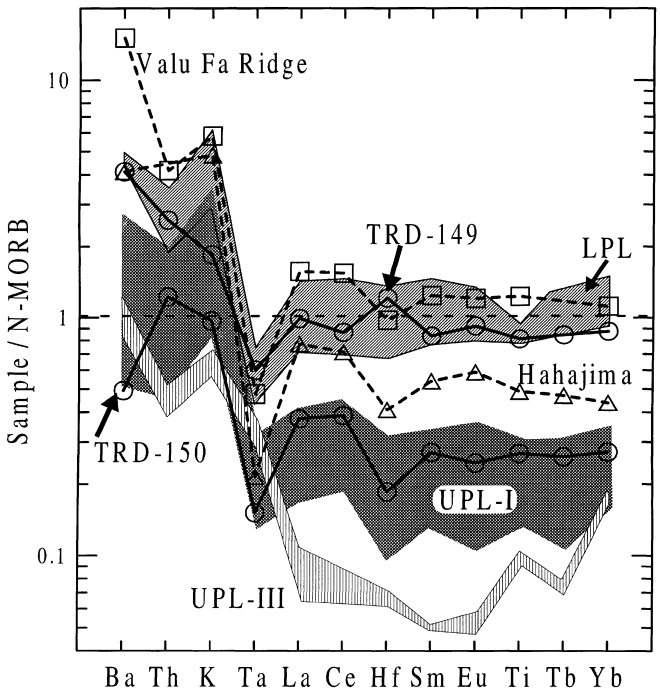

Fig. 3 Trace element compositions of Analiondas rocks. Fields of types I and III UPL picrites (MgO 23.2–35.4 wt% and 31.9–32.8 wt% respectively) after Sobolev et al. (1993). LPL field after Rautenschlein et al. (1985). Bonin forearc tholeiite with ~6.5 wt% MgO (Hahajima Island) after Taylor and Nesbitt (1995). Valu Fa Ridge andesite after Vallier et al. (1991). Normalization to N-MORB (Sun and McDonough 1989)

Clinopyroxene phenocrysts have high-Mg (Mg# = 80–92), high-Cr_2O_3 (up to 1 wt%) and low-TiO_2 (0.15–0.3 wt%) compositions, comparable to those of UPL clinopyroxene phenocrysts (Thy and Xenophontos 1991; Bednarz and Schmincke 1994). However, the Al_2O_3 contents of the TRD-150 clinopyroxene (1.9–3.75 wt%) is slightly higher than those of UPL clinopyroxene at given Mg#. Euhedral clinopyroxene inclusions in olivine phenocrysts and olivine inclusions in clinopyroxene are compositionally similar to phenocrysts.

Euhedral Cr-spinel crystals (up to 300 μm) are abundant as inclusions in olivine, and are rare in clinopyroxene. Spinel included in olivine phenocrysts ranges in Cr# from 28–67, although most are Cr# 55–65. (Table 2, Fig. 4). This variation does not correlate with compositions of host olivine. The entire compositional range of the TRD-150 spinel has lower Cr# than UPL spinel inclusions in olivine (Fig. 4), with the most Cr-rich spinel from TRD-150 being close in composition to the least Cr-rich spinel from the UPL. Also, the range of Cr# in spinel from TRD-150 is ~3 times greater than that in the entire UPL sequence, but comparable to that of the MORB spinel spectrum. TiO_2 contents in spinel inclusions in TRD-150 also show significant variations (0.14–0.65 wt%) which are not correlated with the compositions of host olivine. Spinel from TRD-150 cover the whole range of TiO_2 in UPL spinel.

Plagioclase microphenocrysts are zoned and highly calcic (An 91–79).

Melt inclusion studies

Partially crystallized and glassy melt inclusions (up to 250 μm) are common in olivine phenocrysts and microphenocrysts from TRD-150. Glassy inclusions are common in phenocrysts from pillow margins, whereas in

Table 2 Representative compositions of spinel inclusions and their host olivines from picrite TRD-150[a]

Sample	D69/1	D28	D113	D67	E196	D147/1	D62	D102/2	D133
Host olivine									
SiO_2	38.97	39.84	40.29	39.70	40.39	40.55	40.24	40.83	40.37
FeO[b]	16.02	11.73	9.93	9.83	9.50	9.31	9.13	8.90	7.97
MgO	44.80	47.61	48.90	48.97	48.67	49.37	49.54	49.68	50.45
CaO	0.20	0.22	0.27	0.28	0.23	0.25	0.29	0.25	0.25
Total	99.99	99.40	99.39	98.78	98.79	99.48	99.20	99.66	99.04
Fo	83.29	87.86	89.77	89.88	90.13	90.43	90.63	90.87	91.86
Spinel inclusions									
TiO_2	0.24	0.31	0.31	0.18	0.65	0.22	0.23	0.14	0.17
Al_2O_3	15.62	22.31	17.38	27.03	39.94	24.55	31.63	18.99	20.45
Cr_2O_3	43.90	41.51	48.23	37.26	23.07	40.53	34.37	47.67	47.21
FeO[b]	28.51	21.13	19.54	18.93	15.50	18.67	15.81	17.42	15.62
MnO	0.16	0.25	0.19	0.13	0.13	0.16	0.22	0.22	0.12
MgO	10.35	13.79	13.78	15.26	19.25	15.63	17.56	14.77	15.74
NiO	0.09	0.06	0.13	0.10	0.17	0.20	0.20	0.08	0.09
ZnO	0.12		0.06	0.02		0.05	0.01	0.02	0.05
Total	98.99	99.36	99.62	98.91	98.71	100.01	100.03	99.31	99.45
FeO	18.37	14.39	13.60	12.67	9.15	11.94	10.09	12.16	11.00
Fe_2O_3	11.27	7.49	6.60	6.96	7.05	7.49	6.35	5.85	5.13

[a] Mineral compositions were determined with a Camebax microbeam and a Cameca SX50 electron microprobe at Vernadsky Institute, the University of Tasmania, Hobart, and GEOMAR, Kiel using routine operating conditions and olivine CH-1, and spinel UV-126 as standards (Lavrentev et al. 1974). Ferric and ferrous iron in spinel were calculated from electron microprobe analyses assuming perfect stoichiometry

[b] Total iron as FeO

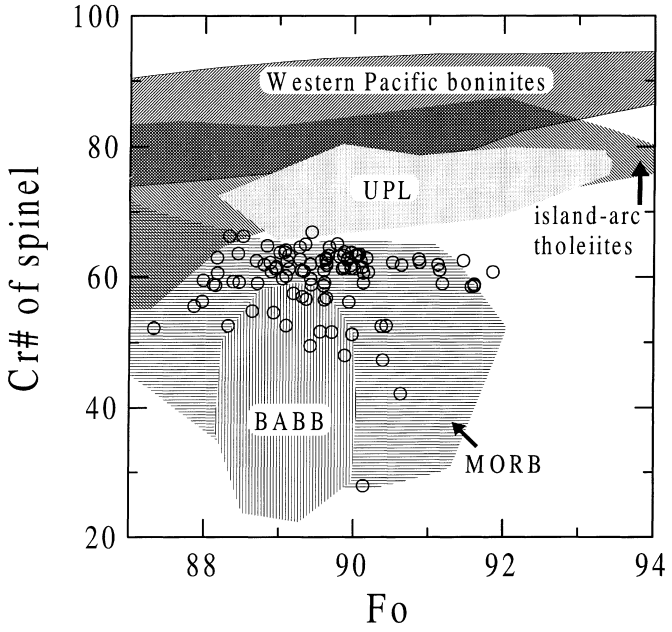

Fig. 4 Compositions of spinel inclusions in olivine from picrite TRD-150 (*open circles*). Compositional field of spinel inclusions in olivine from Troodos upper pillow lavas, types UPL-I and UPL-III, after Sobolev et al. (1993); western Pacific boninites after Sobolev and Danyushevsky (1994), Sigurdsson et al. (1993), and Danyushevsky, unpublished data; primitive island-arc tholeiites after Sigurdsson et al. (1993), Monzier et al. (1993), Allan (1994), and Danyushevsky, unpublished data; primitive mid-ocean ridge picrites and basalts (MORB) after Dmitriev et al. (1991), Sobolev et al. (1989), Kamenetsky (1996), and Danyushevsky and Kamenetsky, unpublished data; back-arc basin basalts (BABB) after Sigurdsson et al. (1993), and Danyushevsky and Kamenetsky, unpublished data. Cr# = 100*[Cr/(Cr + A1)]

central parts of pillows melt inclusions always consist of daughter crystals of clinopyroxene and amphibole in highly evolved dacitic glass. Some 90% of melt inclusions contain daughter sulphide globules. Low density fluid inclusions (up to 150 μm) also present in olivine provide evidence for magma fluid-saturation during crystallization.

Melt inclusions provide an opportunity to extend our data on the melt compositions beyond the range covered by pillow-rim glasses towards more primitive compositions. Also, an experimental study of melt inclusions can establish magma crystallization temperatures.

Technique

Two kinds of experimental studies of melt inclusions have been done using a low-inertia heating stage (Sobolev and Slutskii 1984). Homogenization experiments were carried out following the technique of Sobolev and Danyushevsky (1994), which is directly applicable to the fluid-saturated melts. Inclusions were exposed to temperatures >1100 °C for less than 5 min. In each experiment, inclusions were homogenized and quenched immediately after homogenization. Homogenization was considered to be that moment when daughter silicate crystals were melted and the fluid bubble disappeared inside inclusions. Following Sobolev and Danyushevsky (1994), homogenization temperatures were accepted as temperatures of crystallization (*T*c) for individual crystals. A total of 26 successful homogenization experiments has been done.

Another experimental technique included rapid (<2 min) reheating of melt inclusions up to temperatures within the range established in homogenization experiments, with subsequent quenching. Heating was conducted till the moment of complete melting of the daughter crystals inside inclusions. This technique cannot provide *T*c and absolute concentrations of elements, but can be used to improve statistics on the ratios of elements incompatible in olivine. We employed this simpler method because of the scarcity of naturally quenched glassy melt inclusions in this sample. Representative compositions of homogenized and quickly reheated melt inclusions are shown in Table 3.

Results

Homogenization was successfully achieved in olivine $Fo_{85.8–91.7}$ at temperatures between 1145 and 1210 °C (Fig. 5), and a general positive correlation exists between host-mineral compositions and *T*c, which are substantially lower than those for UPL olivine for a given Fo (Fig. 5). Also, an obvious difference exists in the slopes of Fo-*T* trends between TRD-150 and UPL olivine.

Calculated Kd Fe^{2+}-Mg olivine-melt values (Table 3) for homogenized inclusions vary between 0.31 and 0.38 with no relation to the composition of host olivine. The entire range of Kd values is higher than expected for olivine-melt equilibria in anhydrous or H_2O-bearing basaltic systems ~0.3 (e.g., Roeder and Emslie 1970; see Sobolev and Danyushevsky 1994 for discussion). According to Danyushevsky et al. (1992), this reflects re-equilibration of melt inclusions with their host olivine at lower temperatures, resulting in lower FeO contents of melt inclusions compared to the initially trapped compositions. Such 'iron-loss' by melt inclusions in olivine is

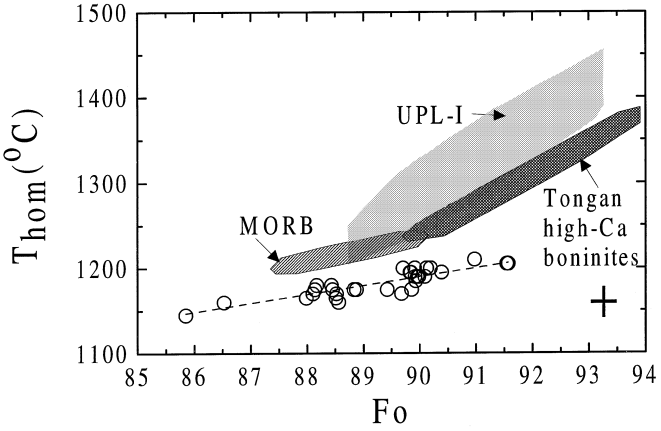

Fig. 5 Temperatures of homogenization of melt inclusions in olivine from picrite TRD-150. The relationships between homogenization temperatures of melt inclusions and compositions of host olivine are shown as fields for Troodos upper pillow lavas, type UPL-I (Sobolev et al. 1993), Tongan high-Ca boninites (Sobolev and Danyushevsky 1994) and MORB from Vema fracture zone, Atlantic (Sobolev et al. 1989). Note the difference in the slope of trends for olivine-only crystallization (UPL-I and Tongan boninites) and olivine + plagioclase ± clinopyroxene cotectic (MORB). The slopes of MORB and TRD-150 crystallization trends are similar

Table 3 Compositions of homogenized and rapidly reheated and quenched melt inclusions in olivine[a]

	1	2	3	4	5	6	7	8	9	10	11	12	13	14	15	16	17	18
	Homogenized inclusions											Rapidly reheated and quenched inclusions						
Sample	OL187	OL236	OL171	OL201	OL239-A	OL237	OL198	OL168	OL10/5	OL153-A	OL10/3	Ol261-B	OL261-A	OL23	OL254	OL191	OL10/2-A	OL10/2-B
SiO_2	50.27	51.21	50.59	51.84	52.38	50.96	50.86	51.36	51.65	50.83	50.78	50.92	50.46	51.62	52.31	53.83	51.47	49.79
TiO_2	0.39	0.47	0.42	0.54	0.81	0.44	0.52	0.43	0.52	0.59	0.72	0.41	0.37	0.88	0.70	1.07	0.26	0.17
Al_2O_3	15.77	15.59	15.03	15.39	16.15	15.15	16.30	16.45	15.67	15.39	15.90	16.07	16.00	15.06	15.85	14.50	14.69	15.63
FeO[b]	5.29	5.35	5.70	5.89	5.86	6.60	6.16	5.98	6.62	7.78	8.25	4.58	5.12	6.51	6.97	7.69	6.13	6.35
MnO	0.11	0.13	0.00	0.10	0.19	0.16	0.15	0.11	0.14	0.04	0.18	0.09	0.12	0.20	0.15	0.18	0.10	0.05
MgO	10.50	10.61	10.67	9.51	9.20	9.75	8.48	9.00	8.86	8.62	7.75	9.73	10.61	9.90	9.25	8.60	12.98	12.73
CaO	14.14	13.59	13.71	13.24	12.75	13.47	13.90	12.99	12.73	12.32	11.69	15.05	14.42	10.05	11.44	9.20	13.11	13.40
Na_2O	1.32	1.35	1.13	1.31	1.75	1.26	1.28	1.28	1.40	1.48	1.86	1.10	1.05	2.20	1.89	2.50	1.13	0.94
K_2O	0.15	0.08	0.10	0.11	0.09	0.17	0.07	0.37	0.06	0.09	0.11	0.11	0.12	0.12	0.11	0.15	0.01	0.01
H_2O	1.41				0.74			1.43			1.83		1.29			1.36	1.46	1.45
Total	99.35	98.38	97.35	97.93	99.92	97.96	97.72	99.40	97.65	97.14	99.07	98.06	99.56	96.54	98.67	99.08	100.34	99.52
Fo	91.57	91.55	90.97	89.92	89.86	89.83	89.68	89.42	87.98	86.52	85.85	91.61	91.61	88.27	88.31	86.72	90.81	90.85
T °C	1205	1205	1210	1190	1175	1195	1170	1175	1165	1160	1145	1200	1200	1195	1190	1190	1270	1270
Kd[c]	0.369	0.370	0.375	0.366	0.358	0.338	0.320	0.360	0.369	0.349	0.313							
SiO_2	51.11	51.84	51.74	52.75	52.65	51.91	52	52.26	52.71	52.19	52.16							
TiO_2	0.40	0.48	0.43	0.55	0.81	0.45	0.53	0.44	0.53	0.61	0.74							
Al_2O_3	16.03	15.78	15.37	15.66	16.23	15.43	16.67	16.74	15.99	15.8	16.33							
FeO[b]	6.16	6.15	6.65	6.58	6.40	7.02	6.30	6.59	7.34	8.32	8.48							
MnO	0.11	0.13	0.00	0.1	0.19	0.16	0.15	0.11	0.14	0.04	0.18							
MgO	10.23	10.33	10.45	9.35	8.96	9.77	8.67	8.87	8.71	8.66	7.96							
CaO	14.38	13.76	14.02	13.47	12.82	13.72	14.21	13.22	12.99	12.65	12.01							
Na_2O	1.34	1.37	1.16	1.33	1.76	1.28	1.31	1.3	1.43	1.52	1.91							
K_2O	0.15	0.08	0.1	0.11	0.09	0.17	0.07	0.38	0.06	0.09	0.11							
*T*dry	1231	1234	1235	1209	1206	1220	1185	1198	1193	1195	1182							
Fe_2O_3	0.8	0.8	0.87	0.86	0.83	0.92	0.82	0.86	0.96	1.09	1.11							
FeO	5.44	5.43	5.87	5.81	5.65	6.19	5.56	5.82	6.48	7.34	7.48							

[a] Melt inclusions were analyzed with a Camebax microbeam and a Cameca SX50 electron microprobe at Vernadsky Institute, the University of Tasmania, Hobart, and GEOMAR, Kiel using routine operating conditions and basaltic glass USNM 111240/52 (Jarosevich et al. 1980) as a standard. H_2O contents were measured using an ion probe Cameca IMS-3f (CRPG, Nancy, France). The details of the technique are given in Sobolev and Chaussidon (1996)

[b] Total iron as FeO

[c] Kd Fe^{2+}-Mg olivine-melt values

common for primitive subduction-related magmatic suites (e.g., Sobolev and Danyushevsky 1994) and can be reversed by a simple calculation (see Danyushevsky et al. 1992 for details), which includes atom by atom exchange of Fe^{2+} and Mg between melt inclusion and host olivine. Such adjustment of melt inclusion compositions does not affect ratios of elements incompatible in olivine and mainly changes the absolute FeO contents of the inclusions. Recalculated melt compositions are shown in Table 3 and are plotted on Figs. 2 and 6.

Inclusions cover a substantial range of MgO (8–10.5 wt%) and a general correlation exists between Fo and MgO, CaO, TiO_2 (positive), and FeO (negative) (Fig. 6). Other elements show no correlation with Fo, and significant variations exist at a given Fo, for both major element contents, and ratios of elements incompatible in olivine (e.g., K_2O/TiO_2, TiO_2/Al_2O_3, CaO/Al_2O_3, Fig. 7).

Inclusions have significant H_2O abundances (0.8–1.8 wt%, Table 3) similar to those of Troodos basaltic glasses (e.g., Muenow et al. 1990; Danyushevsky et al. 1993) and melt inclusions in UPL olivine phenocrysts (Sobolev and Chaussidon 1996).

Basaltic pillow-rim glasses from the Analiondas suite are compositionally close to the least magnesian end of the inclusion range and fall within this range for each major element (Fig. 2). Melt inclusion compositions are significantly different from those of the UPL, implying different parental melts and different crystallization paths. In particular, completely different slopes and starting points are evident on plots of Fo (or MgO, Fig. 2) vs MgO, CaO, FeO and Al_2O_3 (Fig. 6). Compositions of melt inclusions in UPL picrites are consistent with olivine-only (+minor spinel) crystallization until Fo_{88}, whereas TRD-150 melts

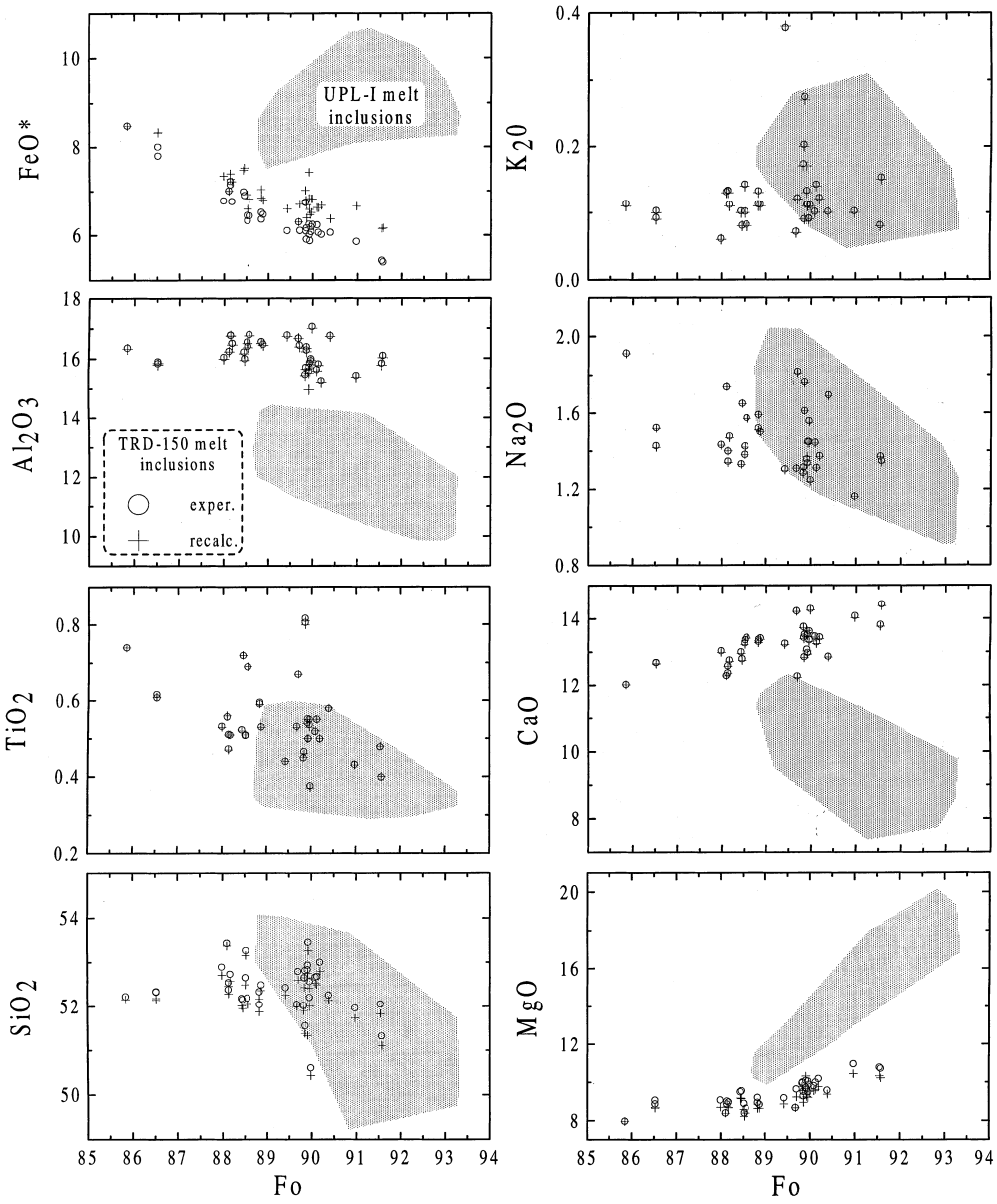

Fig. 6 Relationships between compositions of homogenized melt inclusions and their host olivines in TRD-150. There are no substantial differences (apart from FeO) between experimental compositions and those recalculated to account for "iron-loss" (see text for details). The field of melt inclusions in olivine from Troodos upper pillow lavas, type UPL-I is after Sobolev et al. (1993)

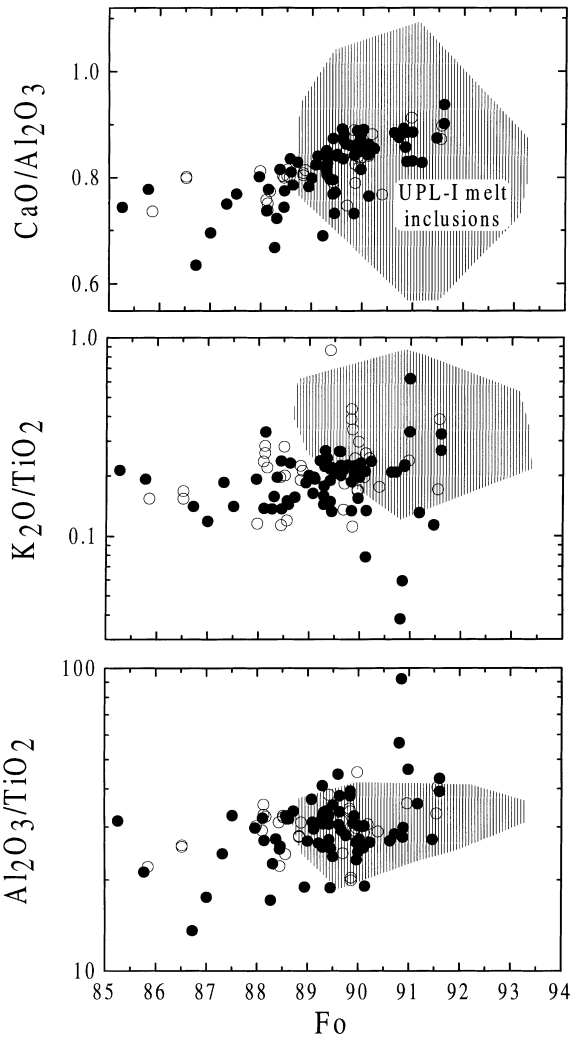

Fig. 7 Compositions of melt inclusions in olivine from sample TRD-150 compared with those in olivines from UPL-I (*shaded area*, after Sobolev et al. 1993). *Open circles* homogenized melt inclusion, *filled circles* rapidly reheated and quenched melt inclusions. Note large variations in ratios of elements incompatible in olivine at a given Fo

demonstrate decreasing CaO with decreasing MgO and Fo for the entire range of olivine compositions. The range of Na_2O, TiO_2 and K_2O variations is similar in melt inclusions from TRD-150 and UPL picrites (Fig. 6).

Discussion

Genetic relationships between primitive and evolved LPL

Our study of fresh primitive lavas from the lowest parts of the Troodos extrusive sequence (Analiondas suite) clearly demonstrates that they are parental to the LPL andesites and dacites, as was previously proposed by Bednarz and Schmincke (1994).

Overall, melt inclusions and volcanic glasses form a trend extending from high-MgO basaltic through andesitic to dacitic compositions of the LPL (Fig. 2), and trace element contents in the most evolved Analiondas glass TRD-149 are identical to the LPL andesites and dacites from other areas (Fig. 3). The fractionation trend defined by major elements suggests early olivine-clinopyroxene cotectic crystallization from Analiondas parental melts, since CaO decreases with decreasing MgO (Fig. 2, 6) from the earliest recorded stages of fractionation. This is also supported by the presence of magnesian (up to Mg# 92) clinopyroxene phenocrysts in the rock and numerous inclusions of olivine in clinopyroxene phenocrysts and vice versa, and by a correlation between decreasing Fo and Ca contents in olivine phenocrysts. Moreover, the Fo-Tc trend (Fig. 5) for Analiondas olivines is shallower than expected for olivine-only crystallization (cf. UPL and Tonga high-Ca boninite olivines) and similar to those of cotectic suites (cf. MORB olivines).

However, crystallization of olivine and pyroxene alone cannot explain major element variations along the fractionation path. A simple calculation based on differences in CaO between the most primitive and the most evolved inclusions suggests at least 25% of olivine + clinopyroxene crystallization, which would produce an Al_2O_3 content of at least 20 wt% in the evolved inclusions; this is significantly higher than observed values (16–17 wt%, Fig. 2). Least square linear approximation calculations (Wright and Doherty 1970) suggest that the least-magnesian melt inclusion compositions (MgO ~8 wt%) can be produced from primitive melts (MgO ~10.3 wt%) by 44.8 wt% crystallization of olivine, clinopyroxene, and plagioclase in proportions 3.9:21.8:18.4 (Table 4), which are consistent with

Table 4 Crystal fractionation between primitive and evolved melt inclusion compositions in olivine TRD-150

	Ol	Cpx	Plag	Evolved melt	Primitive melt	Calculated primitive melt
SiO_2	40.21	53.76	46.58	52.91	51.63	51.58
TiO_2		0.1		0.73	0.40	0.43
Al_2O_3		1.98	32.44	16.21	15.53	15.54
FeO	11.07	4.14	1.04	8.42	6.22	6.24
MgO	48.44	18.27	0.12	7.90	10.33	10.34
CaO	0.28	21.66	16.83	11.92	14.53	14.54
Na_2O		0.09	1.62	1.90	1.35	1.38
Amount	0.039	0.218	0.184	0.559		1.000

petrographic and experimental cotectic proportions (e.g., Thy and Xenophontos 1991). Compositions of olivine ($Fo_{88.6}$) and clinopyroxene (Mg# 88.7) correspond to average compositions for the fractionation interval covered, and the best fit was obtained using plagioclase An_{85} (sum of squares of residuals = 0.003 wt%). As the most calcic plagioclases found in TRD-150 are An_{91}, we consider the results obtained as being quite reasonable. Most likely, plagioclase started to crystallize later than olivine and clinopyroxene and appeared on the liquidus at ~9 wt% MgO where, despite a significant scatter (Fig. 2), the increase in Al_2O_3 appears to halt, and FeO begins to rise during melt evolution.

Significant variations in compositions of melt and spinel inclusions at a given Fo (Figs. 6, 7, 4) may suggest periodic replenishment of a continuously evolving magma chamber with primitive melts (O'Hara 1977). If the mixing of primitive and evolved magmas had occurred, then the integrated fractionation trend would differ substantially from that of the closed system. This, for example, can account for the observed variations in CaO/Al_2O_3 values and Al_2O_3 contents in melt inclusions at a given Fo (Fig. 7, 6), and for variations in compositions of volcanic glasses at a given MgO (Fig. 2).

However, large variations of Na_2O, TiO_2 and particularly K_2O in melt inclusions (Fig. 2, 6, 7) are unlikely to be accounted for by olivine + clinopyroxene ± plagioclase crystallization and mixing between evolved and primitive magmas. Most likely, they reflect an initial variety of parental melts. Melts with substantially different alkalis and TiO_2 appear to be broadly similar in SiO_2, Al_2O_3, CaO, MgO, FeO and have similar temperatures, ruling out mixing of contrasting types of magmas and implying close genetic relations between these melts. Such variation may reflect processes in the mantle during dynamic melting accompanied by variable contribution of subduction-related components (e.g., Pearce et al. 1995).

Mantle source of the LPL primary melts

Data presented in this paper rule out derivation of LPL parental melts by crystallization of any primitive UPL magmas. First, the evolutionary path of Analiondas melts at MgO > 8 wt% differs significantly from that of the UPL with similar MgO in having lower FeO and higher Al_2O_3 and CaO (Fig. 2, 6). Note that all UPL have similar concentrations of these elements. Second, spinel inclusions in LPL olivine have lower Cr# (28–67) compared to UPL spinel inclusions (65–80) at a given Fo (Fig. 4). Third, olivine crystallization temperatures for a given Fo are substantially lower than those for UPL olivines (Fig. 5).

Overall low TiO_2 contents of Analiondas melts (0.4–0.8 wt% at MgO > 9 wt% compared with 0.6–1.1 wt% in MORB at similar MgO) suggest their origin from a relatively refractory mantle source. Liquidus olivine of the most primitive LPL melts (Fo_{92}) is refractory enough to suggest their equilibrium with the mantle (e.g., Green 1970). However, high normative diopside contents of these melts (~38% in the olivine-clinopyroxene-quartz projection of Falloon et al. 1988), a result of their high CaO contents, makes them unlike any experimentally established depleted peridotite-source magmas (e.g., Falloon et al. 1988).

The high-Ca signature may appear via reaction of ascending high-temperature primary UPL-like melts with surrounding cooler (<1250 °C) mantle peridotites. This would lead to cooling of those melts accompanied by dissolution of clinopyroxene from the peridotite and precipitation of olivine and orthopyroxene from the melt, a mechanism similar to that proposed to explain chemical features of some magmatic suites (e.g., Kelemen 1995). However, this process would not significantly affect melt Al_2O_3 contents (due to broadly similar and relatively low Al_2O_3 contents in pyroxenes), and would increase melt Cr/Al ratio (due to high Cr_2O_3 content in clinopyroxene). This is inconsistent with relatively high-Al_2O_3 contents of parental LPL magmas compared to the UPL at similar MgO (Fig. 2), and with lower Cr# of LPL spinels.

Our preferred explanation is that the high-Ca contents result from ~10% of early olivine fractionation from primary melts, not recorded in the sample studied (i.e., olivine phenocrysts which crystallized during first 10% of crystallization of primary melts (Fo > 92) are not present in our samples). If so, normative diopside content of the primary melt was ~30%, consistent with the results of mantle melting experiments. In this case, primary melts should have had temperatures of ~1300 °C, MgO ~14.5 wt%, and Fo_{94} liquidus olivine. They will be in equilibrium with the mantle at ~10 kbar (Falloon et al. 1988).

A comparison of the LPL and UPL mantle sources

A similar petrological approach which involved experimental studies of melt inclusions in olivine and analyses of volcanic glasses, has been employed by Sobolev et al. (1993) to establish primary melt compositions of the UPL. Their results indicate that UPL primary melts contained 19–22 wt% MgO, had liquidus olivine $Fo_{93–94}$, and according to high-pressure experimental studies, they were formed in the mantle at 15–18 kbar, 1430–1480 °C (Danyushevsky et al. 1994).

A comparison of generation conditions of the LPL (this study) and UPL (Sobolev et al. 1993; Danyushevsky et al. 1994) primary melts clearly demonstrates that they could not be formed by progressive depletion of a single mantle source, as was previously suggested (e.g., Bednarz and Schmincke, 1994), and supports the multi-source model of Sobolev et al. (1993). Indeed, temperature differences between source regions (~150 °C over 5–8 kbar), position of these sources within the mantle wedge (~10 kbar for the colder LPL source vs 15–18 kbar for the UPL source), and temporal succession of

Troodos volcanism, cannot all be reconciled in the framework of existing models of mantle wedge processes, thermal structure and evolution, if a single mantle source is invoked (e.g., Davies and Stevenson 1992).

An additional argument in support of two independent mantle sources is the similarity of Al_2O_3/TiO_2 values in the LPL and UPL primitive magmas (Fig. 7), as this ratio is sensitive to the overall source depletion and should be higher in the UPL if they were formed from the residue after LPL extraction.

We also note that evidence for distinct mantle sources cannot be retrieved when compositions of the evolved (MgO < 8 wt%) rocks and glasses are considered, as all initial differences in melt compositions are masked by the Assimilation and Fractional Crystallization (AFC) processes (Fig. 2). Moreover, incompatible element signatures of SSZ magmas are mainly controlled by subduction-related component(s) (e.g., McCulloch and Gamble 1991), and thus can be similar in magmas produced from distinct mantle sources in a single SSZ. This can explain the general similarity in trace-element characteristics between primitive LPL and UPL (Fig. 3).

A comparison of the LPL mantle sources with those of tholeiites from well-developed intra-oceanic arcs

LPL andesites and dacites have been recognized as island-arc tholeiites (e.g., Robinson et al. 1983; Schmincke et al. 1983) due to their geochemical and isotopic similarity to evolved rocks dominating magmatic assemblages in well-developed intra-oceanic arcs. However, as discussed above, the compositions of these evolved rocks retain little information about mantle sources which can be obtained when the compositions of primitive melts are available. Thus, our data on primitive LPL allow reassessment of this classification by comparing them to primitive arc tholeiites. To avoid overprint of subduction-related components on SSZ magma compositions, we use compositions of magmatic spinel, which are unaffected by subduction-related components, and reflect degree of depletion of the mantle source in basaltic component (e.g., Dick and Bullen 1984; Arai 1992). Limited data on spinels in rare primitive tholeiites in well-developed island arcs (Vanuatu, Hunter Ridge and Tonga) are compiled in Fig. 4 together with other low-K magmatic suites from SSZ and MOR. The obvious similarity between island-arc tholeiite and UPL spinels suggests that the mantle sources of their parental magmas were similarly depleted, whereas LPL spinels are comparable with those from MORB and BABB and are significantly less Cr-rich than those in arc tholeiites. This strongly suggests that primitive LPL melts were formed from a mantle source which was more fertile than that of tholeiites from well-developed intra-oceanic arcs, but broadly similar in its fertility to that of MORB and BABB. The higher degrees of melting during formation of the LPL primary melts compared to average MORB, as implied by lower Ti contents and high Fo of liquidus olivine, were probably caused by the presence of subduction-related components (H_2O).

Possible modern analogs for the Troodos ophiolite

Our results indicate some important differences between the Troodos ophiolite and modern forearcs. The variety of magmatic suites within modern forearcs (i.e., boninite-arc tholeiite compositional spectrum) is believed to arise from along-strike variations in the crustal extension rates and mantle-wedge temperatures (Taylor and Nesbitt 1995; Bloomer et al. 1995), with boninites produced during more intensive spreading. Troodos boninites (UPL), in contrast, were formed after the main extensional phase as recorded by the late UPL-related dykes in the Dyke Complex (e.g., Desmons et al. 1980, Dilek et al. 1990). Moreover, most forearc spreading-related boninites belong to the low-Ca subtype (Crawford et al. 1989), whereas Troodos boninites are high-Ca, implying more refractory mantle sources for the former, consistent with higher Cr# of their spinels (Fig. 4) and lower contents of incompatible elements at a similar degree of fractionation (e.g., Crawford et al. 1989).

The mantle source which produced high-Ca boninites on Troodos (UPL) was significantly hotter than that of the tholeiites (LPL) (Sobolev et al. 1993). However, even though the boninite-tholeiite association is a typical feature of all SSZ ophiolites and forearcs (e.g., Wood et al. 1982; Bloomer 1987; Crawford and Keays 1987; Flower and Levine 1987; Taylor et al. 1992; Bedard et al. 1994), the presence of distinct mantle sources during forearc magmatism cannot be readily assumed, as it has been suggested that different boninite suites may be generated under completely different conditions (e.g., Danyushevsky et al. 1995). The common feature of all boninites, a refractory mantle source metasomatized by an H_2O-bearing component(s), is not sufficient to constrain their genesis.

It is also difficult to evaluate whether the generation conditions of the LPL primary magmas and compositions of their mantle source resemble those of tholeiites from modern forearcs. Major and trace-element compositions of relatively primitive basaltic rocks from the Bonin forearc (Hahajima Is., Taylor and Nesbitt 1995) closely resemble those of primitive LPL (Figs. 2, 3). However, our study of Troodos lavas demonstrates that compositions of samples with MgO < 8 wt% can be similar in suites with different primary magmas due to the AFC processes and the dominance of subduction-related components in their trace-element compositions. Thus, the question as to whether forearc tholeiites are similar to the LPL and originate from a mantle source different from that of island-arc tholeiites, remains open.

It appears that some similarity exists between magmatic suites of the Troodos Ophiolite and those erupted at the southern tip of the Valu Fa Ridge suggesting that

propagation of a backarc spreading centre into the subarc lithosphere is another possible setting for Troodos magmatism. Importantly, andesites of the Valu Fa Ridge with strong "arc" compositional signature (Vallier et al. 1991) are erupted in the spreading environment, and more primitive lavas resembling high-Ca boninites are found from adjacent off-axis non-spreading seamounts (Frenzel et al. 1990). However, despite a general similarity between Valu Fa Ridge and LPL andesites in major and trace element compositions (Figs. 2, 3), the lack of data on more primitive Valu Fa spreading-related lavas and on exact temporal relationships between them and high-Ca lavas, precludes any definite conclusions on their origin.

Another combination of broadly contemporaneous backarc tholeiites and high-Ca boninites associated with propagation of backarc spreading into arc lithosphere, has been described from the northern termination of the Tonga Ridge (e.g., Falloon and Crawford 1991; Danyushevsky et al. 1995). The Tongan high-Ca boninites, similar to the UPL in compositions of primary melts and *PT* parameters of their origin in the mantle (Sobolev et al. 1993; Sobolev and Danyushevsky 1994; Danyushevsky et al. 1995), are formed as hot residual Samoan plume mantle intruded above the slab and subsequently re-melted due to interaction with the subduction-related component (Danyushevsky et al. 1995). Hot refractory plume-related mantle above the slab was also inferred as a source of Troodos UPL (Sobolev et al. 1993). Although little is known about spreading-related lavas erupted at the propagation tip, relatively high H_2O contents in glasses from the adjacent King's Triple Junction (Danyushevsky et al. 1993) imply likely "arc" affinities, and thus possible compositional similarities to the LPL.

Acknowledgements The authors gratefully acknowledge support and assistance of the Geological Survey Department of Cyprus during field trips in 1989 and 1993. Our special thanks go to A.V. Sobolev, L.V. Dmitriev, and O.P. Tsamerian from the Vernadsky Institute, Russian Academy of Science, for continuous support and useful discussion over the years. We are also grateful to A.J. Crawford for useful discussions, critical comments, and the usual patience in correcting English. We thank T.L. Grove, N. Rogers and one anonymous reviewer for critical comments on this paper which significantly improved the original manuscript. This research was supported by the Russian Foundation for Basic Research grants 96-05-66014, 97-05-65909 and Volkswagen Stiftung Foundation (Grant I/68-569) to MVP; by Australian Research Council through Large Grants to LVD and A.J. Crawford, and Postdoctoral Fellowship to LVD; by RSES (ANU) through funding to VSK. We acknowledge support of Museum of Natural History, Washington DC, which provided electron microprobe standards.

References

Allan JF (1994) Cr-spinel in depleted basalts from the Lau basin backarc: petrogenetic history from Mg-Fe crystal-liquid exchange. Proc Ocean Drill Prog Sci Res 135: 565–583

Arai S (1992) Chemistry of chromian spinel in volcanic rocks as a potential guide to magma chemistry. Mineral Mag 56: 173–184

Bailey DG, Langdon GS, Malpas J, Robinson PT (1991) Ultramafic and related lavas from the Margi area, Troodos ophiolite. Geol Surv of Can Pap 90–20: 187–202

Bedard JH, Hebert R, Varfalvy V, Melancon B (1994) Boninite magmatism in the Bay of Islands ophiolite. Eos Trans Am Geophys Union 75: F731

Bednarz U, Schmincke H-U (1994) Petrological and geochemical evolution of the Northeastern Troodos Extrusive Series, Cyprus. J Petrol 35: 489–523

Bednarz U, Gotte P, Schmincke H-U (1991) Petrography of altered submarine extrusive rockes and major element mobility in Cyprus drill-holes CY-1 and CY-1A. Geol Surv Can Pap 90–20: 95–116

Bloomer SH (1987) Geochemical characteristics of boninite- and tholeiite-series volcanic rocks from the Mariana forearc and the role of an incompatible element-enriched fluid in arc petrogenesis. Geol Soc Am Spec Pap 215: 151–164

Bloomer SH, Hawkins JW (1983) Gabbroic and ultramafic rocks from the Mariana Trench: an island arc ophiolite. In: Hayes DE (ed) The tectonic and geological evolution of the SE Asian seas and islands, Pt 2 (AGU Monograph 27). American Geophysical Union, Washington DC, pp 294–317

Bloomer SH, Taylor B, MacLeod CJ, Stern RJ, Fryer P, Hawkins JW, Johnson L (1995) Early arc volcanism and the ophiolite problem: a perspective from drilling in the Western Pacific. In: Taylor B , Natland J (eds) Active margins and marginal basins of the Western Pacific. Am Geophys Union, Washington, pp 1–30

Boyle JF, Robertson AHF (1984) Evolving metallogenesis at the Troodos spreading axis. In: Gass IG, Lippard SJ, Shelton AW (eds) Ophiolites and oceanic lithosphere. Geol Soc London Spec Pub 13: 169–181

Cameron WE (1985) Petrology and origin of primitive lavas from the Troodos ophiolite, Cyprus. Contrib Mineral Petrol 89: 239–255

Crawford AJ, Keays RR (1987) Petrogenesis of Victorian Cambrian tholeiites and implications for the origin of associated boninites. J Petrol 28: 1075–1109

Crawford AJ, Falloon TJ, Green DH (1989) Classification, petrogenesis and tectonic setting of boninites. In: Crawford AJ (ed) Boninites. Unwin Hyman, London, pp 1–49

Danyushevsky LV, Sobolev AV, Kononkova NN (1992) Methods of studing magma inclusions in minerals during investigations on water-bearing primitive mantle melts (Tonga trench boninites). Geochem Int 29: 48–62

Danyushevsky LV, Falloon TJ, Sobolev AV, Crawford AJ, Carroll M, Price RC (1993) The H_2O content of basalt glasses from southwest Pacific backarc basins. Earth Planet Sci Lett 117: 347–362

Danyushevsky LV, Green DH, Falloon TJ, Sobolev AV (1994) The compositions of anhydrous and H_2O-undersaturated melts in equilibrium with refractory peridotites at 15 and 20 kb: implications for high-Ca boninite petrogenesis. Mineral Mag 58A: 209–210

Danyushevsky LV, Sobolev AV, Falloon TJ (1995) North Tongan high-Ca boninite petrogenesis: the role of Samoan plume and subduction zone – transform fault transition. J Geodynamics 20: 219–241

Davies JH, Stevenson DJ (1992) Physical model of source region of subduction zone volcanics. J Geophys Res 97B: 2037–2070

Desmons J, Delaloye M, Desmet A, Gagny C, Rocci G, Voldet P (1980) Trace and rare earth element abundances in Troodos lavas and sheeted dykes, Cyprus. Ofioliti 5: 35–56

Dick HBJ, Bullen T (1984) Chromian spinel as a petrogenetic indicator in abyssal and alpine-type peridotites and spatially associated lavas. Contrib Mineral Petrol 86: 54–76

Dilek Y, Thy P, Moores EM, Ramsden TW (1990) Tectonic evolution of the Troodos ophiolite within the Tethyan framework. Tectonics 9: 811–823

Dmitriev LV, Magakian R, Danyushevsky LV, Kamenetsky VS (1991) New data on primitive tholeiites from the Atlantic Ocean (12th cruise of the R/V 'Academic Boris Petrov') (in Russian).

Volcanology and Seismology (Vulkanologia i Seismologia) 6: 78–94
Duncan RA, Green DH (1980) The role of multistage melting in the formation of oceanic crust. Geology 8: 22–26
Duncan RA, Green DH (1987) The genesis of refractory melts in the formation of oceanic crust. Contrib Mineral Petrol 96: 326–342
Falloon TJ, Crawford AJ (1991) The petrogenesis of high-calcium boninites from the north Tonga ridge. Earth Planet Sci Lett 102: 375–94
Falloon TJ, Green DH, Hatton CJ, Harris KL (1988) Anhydrous partial melting of a fertile and depleted peridotite from 2 to 30 kb and application to basalt petrogenesis. J Petrol 29: 1257–1282
Falloon TJ, Malahoff A, Zonenshain LP, Bogdanov Y (1992) Petrology and geochemistry of back-arc basin basalts from Lau Basin spreading ridges at 15, 18 and 19°S. Mineral Petrol 47: 1–35
Flower MFJ, Levine HM (1987) Petrogenesis of a tholeiite-boninite sequence from Ayios Mamas, Troodos ophiolite: evidence for splitting of a volcanic arc? Contrib Mineral Petrol 97: 509–524
Frenzel G, Mühe R, Stoffers P (1990) Petrology of the volcanic rocks from the Lau Basin, southwest Pacific. Geol Jahrb D92: 395–479
Gass IG (1958) Ultrabasic pillow lavas from Cyprus. Geol Mag XCV: 241–251
Gass IG, Smewing JD (1973) Intrusion, extrusion, and metamorphism at constructive margins: evidence from Troodos Massif, Cyprus. Nature 242: 26–29
Green DH (1970) The origin of basaltic and nephelinitic magma. Trans Leicester Lit Phil Soc 64: 28–54
Jarosewich EJ, Nelen JA, Norberg JA (1980) Reference samples for electron microprobe analysis. Geostandards Newsletter 4: 43–47
Kamenetsky V (1996) Methodology for the study of melt inclusions in Cr-spinel, and implications for parental melts of MORB from FAMOUS area. Earth Planet Sci Lett 142: 479–486
Kelemen PB (1995) Genesis of high Mg# andesites and the continental crust. Contrib Mineral Petrol 120: 1–19
Lavrentev YG, Pospelova LN, Sobolev NV (1974) Rock-forming mineral compositions determination by X-ray microanalysis (in Russian). Zavodskaya Laboratoria (in Russian) 40: 657–666
McCulloch MT, Cameron WE (1983) Nd-Sr isotopic study of primitive lavas from the Troodos ophiolite, Cyprus: evidence for a subduction-related setting. Geology 11: 727–731
McCulloch MT, Gamble JA (1991) Geochemical and geodynamical constraints on subduction zone magmatism. Earth Planet Sci Lett 102: 358–374
Monzier M, Danyushevsky LV, Crawford AJ, Bellon H, Cotten J (1993) High-Mg andesites from the southern termination of the New Hebrides island arc. J Volcanol Geotherm Res 57: 193–217
Muenow DW, Garcia MO, Aggrey KE, Bernarz U, Schmincke H-U (1990) Volatiles in submarine glasses as a discriminant of tectonic origin: application to the Troodos ophiolite. Nature 343: 159–161
O'Hara MJ (1977) Geochemical evolution during fractional crystallization of a periodically refilled magma chamber. Nature 266: 503–507
Pearce JA, Lippard SJ, Roberts S (1984) Characteristics and tectonic significance of supra- subduction zone ophiolites. In: Kokelaar BP, Howells MF (Eds) Marginal basin geology. Geol Soc London Spec Pub 16: 77–94
Pearce JA, van der Laan SR, Arculus RJ, Murton BJ, Ishii T, Peate DW, Parkinson IJ (1992) Boninite and harzburgite from Leg 125 (Bonin-Mariana forearc): a case study of magma genesis during the initial stages of subduction. Proc Ocean Drill Prog Sci Res 125: 623-659
Pearce JA, Baker PE, Harvey PK, Luff IW (1995) Geochemical evidence for subduction fluxes, mantle melting and fractional crystallization beneath the South Sandwich island arc. J Petrol 36: 1073–1109
Rautenschlein M, Jenner GA, Hertogen J, Hofmann AW, Kerrich R, Schmincke H-U, White WM (1985) Isotopic and trace element composition of volcanic glasses from the Akaki Canyon, Cyprus: implications for the origin of the Troodos ophiolite. Earth Planet Sci Lett 75: 369–383
Robinson PT, Melson WG, O'Hearn T, Schmincke H-U (1983) Volcanic glass compositions of the Troodos ophiolite, Cyprus. Geology 11: 400–404
Rogers NW, MacLeod CJ, Murton BJ (1989) Petrogenesis of boninitic lavas from the Limassol Forest Complex, Cyprus. In: Crawford AJ (ed) Boninites. Unwin Hyman, London, pp 288–313
Roeder PL, Emslie RF (1970) Olivine-liquid equilibrium. Contrib Mineral Petrol 29: 275–289
Schmincke H-U, Rautenschlein M, Robinson PT, Mehegan JM (1983) Troodos extrusive series of Cyprus: a comparison with oceanic crust. Geology 11: 405–409
Sharaskin AY, Pustchin IK, Zlobin SK, Kolesov GM (1983) Two ophiolite sequences from the basement of the northern Tonga arc. Ofioliti 8: 411–430
Sigurdsson IA, Kamenetsky VS, Crawford AJ, Eggins SM, Zlobin SK (1993) Primitive island arc and oceanic lavas from the Hunter ridge-Hunter fracture zone. Evidence from glass, olivine and spinel compositions. Mineral Petrol 47: 149–169
Sobolev AV, Chaussidon M (1996) H_2O concentrations in primary melts from island arcs and mid-ocean ridges: implications for H_2O storage and recycling in the mantle. Earth Planet Sci Lett 137: 45–55
Sobolev AV, Danyushevsky LV (1994) Petrology and geochemistry of boninites from the north termination of the Tonga Trench: constraints on the generation conditions of primary high-Ca boninite magmas. J Petrol 35: 1183–1211
Sobolev AV, Slutskii AB (1984) Composition and crystallization conditions of the initial melt of the Siberian meimechites in relation to the general problem of ultrabasic magmas. Soviet Geology and Geophysics 25: 93–104
Sobolev AV, Danyushevky LV, Dmitriev LV, Suschevskaya NM (1989) High-alumina magnesian tholeiite as the primary basalt magma at Midocean ridge. Geochem Int 26: 128–133
Sobolev AV, Portnyagin MV, Dmitriev LV, Tsameryan OP, Danyushevsky LV, Kononkova NN, Shimizu N, Robinson PT (1993) Petrology of ultramafic lavas and associated rocks of the Troodos massif, Cyprus. Petrology 1: 331–361
Stern RJ, Bloomer SH (1992) Subduction zone infancy: examples from the Eocene Izu-Bonin-Mariana and Jurassic California Arcs. Geol Soc Am Bull 104: 1621–1636
Sun S-s, McDonough WF (1989) Chemical and isotopic systematics of oceanic basalts: implications for mantle composition and processes. In: Saunders AD, Norry MJ (eds) Magmatism in the ocean basins. Geol Soc London Spec Pub 42: 313–345
Taylor B (1992) Rifting and the volcanic-tectonic evolution of the Isu-Bonin-Mariana Arc. Proc Ocean Drill Prog Sci Res 126: pp 627–651
Taylor RN (1987) The stratigraphy, geochemistry and petrogenesis of the Troodos extrusive sequence, Cyprus. PhD thesis, University of Southampton
Taylor RN, Nesbitt RW (1995) Arc volcanism in an extensional regime at the initiation of subduction: a geochemical study of Hahajima, Bonin Islands, Japan. In: Smellie JL (Ed) Volcanism associated with extension at consuming plate margins. Geol Soc London Spec Publ 81: 115–134
Taylor RN, Murton BJ, Nesbitt RW (1992) Chemical transects across intra-oceanic arcs: implications for the tectonic setting of ophiolites. In: Parson LM, Murton BJ , Browning P (eds) Ophiolites and their modern oceanic analogues. Geol Soc London Spec Publ 60: 117–132
Thy P, Xenophontos C (1991) Crystallization orders and phase chemistry of glassy lavas from the pillow sequences, Troodos ophiolite, Cyprus. J Petrol 32: 403–428
Vallier TL, Jenner GA, Frey FA, Gill JB, Davis AS, Volpe AM, Hawkins JW, Morris JD, Cawood PA, Morton JL, Scholl DW, Rautenschlein M, White WM, Williams RW, Stevenson AJ,

White LD (1991) Subalkaline andesite from Valu Fa Ridge, a back-arc spreading center in southern Lau Basin: petrogenesis, comparative chemistry, and tectonic implications. Chem Geol 91: 227–256

Wood DA (1979) Dynamic partial melting: its application to the petrogeneses of basalts erupted in Iceland, the Faeroe Islands, the Isle of Skye (Scotland) and the Troodos Massif (Cyprus). Geochim Cosmochim Acta 43: 1031–1046

Wood DA, Marsh NG, Tarney J, Joron J-L, Fryer P, Treuil M (1982) Geochemistry of igneous rocks recovered from a transect across the Mariana Trough, arc, fore-arc, and trench sites 453 through 461, Deep Sea Drilling Project Leg 60. Initial Rep Deep Sea Drill Proj 60: 611–645

Wright TL, Doherty PC (1970) A linear programming and least squares computer method for solving petrologic mixing problems. Geol Soc Am Bull 81: 1995–2008